

Chapter 2

Interatomic Bonding

In computational nanoscale science, we deal with many body nanostructures of all types composed of N atoms or molecules. The value of N can range from several hundred to several billions. To handle the energetics of these structures computationally, the most efficient way is to express the total interaction energies in these systems in terms of interatomic potentials that are functions of the atomic coordinates. The reason is that, even with the high-performing computing platforms and sophisticated simulation techniques available today, the existing quantum mechanical-based, or ab initio, strategies can handle nanoscale systems composed of, at most, a few hundred atoms. Interatomic potential energy functions will, therefore, be indispensable in modeling and simulation studies for a long time to come.

2.1 Potential Energy Function (PEF)

The total potential energy function, H_I of an N -body nanostructure, refers to the configurational potential energy that can be expressed in terms of the position coordinates r of its constituent atoms. The simplest way is to express this energy as a cluster expansion involving two, three-body etc. The total potential energy functions H_I is as follow,

$$H_I = \frac{1}{2!} \sum_i \sum_{j \neq i} V_2(\mathbf{r}_i, \mathbf{r}_j) + \frac{1}{3!} \sum_i \sum_{j \neq i} \sum_{k \neq i, j} V_3(\mathbf{r}_i, \mathbf{r}_j, \mathbf{r}_k) + \dots \quad (2.1)$$

where V_n are n -body interatomic potential functions. In (Eq. 2.1), V_2 is the pair-wise potential between atoms i and j , and V_3 is the three-body potential involving atoms i , j and k .

Potential energy functions that are constructed should satisfy a set of criteria so that they are effective in computational modeling applications. Brenner [1] has succinctly summarized the critical properties that a potential energy function must possess. The properties are as follows:

- (1) Flexibility. A PEF must be sufficiently flexible that it accommodates as wide a range as possible of fitting data. For solid systems, the data might include crystalline lattice constants, cohesive energies, elastic properties, vacancy formation energies and surface energies.
- (2) Accuracy. A PEF should be able accurately to reproduce an appropriate fitting database.
- (3) Transferability. A PEF should be able to describe, at least qualitatively, if not with quantitative accuracy, structures that were not included in the fitting database.
- (4) Computational efficiency. Evaluation of the PEF should be relatively efficient, vis-à-vis such quantities as the system size and time-scale of interest, as well as the available computing resources.

In this chapter, we present a rather thorough description of most of the state-of-the-art PEFs that have been developed and used in the computational modeling of the mechanical, thermal, structural, transport and storage properties of carbon nanotubes. These potentials have been extensively used in many simulation studies. In the early molecular mechanics studies in both inorganic and organic chemistry the strain energy, U_{total} is defined as arising from four principle energy terms (Eq. 2.2),

$$U_{\text{total}} = \sum_{\text{molecule}} (E_b + E_\theta + E_\phi + E_{nb}) \quad (2.2)$$

where $\sum E_b$ is the total bond deformation energy, $\sum E_\theta$ the total valence angle deformation energy, $\sum E_\phi$ the total torsional (or dihedral) angle deformation energy and $\sum E_{nb}$ the total nonbonded (van der Waals) interaction energy. The individual energy terms are calculated using simple functions. Bonds are modeled as elements that obey Hooke's law (Eq. 2.3),

$$E_b = \frac{1}{2} k_b (r_{ij} - r_0)^2 \quad (2.3)$$

Where k_b is the force constant or spring 'strength' and r_0 is the ideal bond length or the preferred spring's length. Valence angles are modeled in a very similar way (Eq. 2.4),

$$E_\theta = \frac{1}{2} k_\theta (\theta_{ij} - \theta_0)^2 \quad (2.4)$$

where k_θ is the strength of the 'spring' holding the angle at its ideal value of θ_0 .

Torsion or dihedral angles cannot be modeled in the same manner since a periodic function is required (Eq. 2.5),

$$E_\phi = \frac{1}{2}k_\phi(1 + \cos(m(\phi_{ijkl} + \phi_{\text{offset}}))) \quad (2.5)$$

where k_ϕ is the height of the barrier to rotation about the torsion angle ϕ_{ijkl} , m is the periodicity and ϕ_{offset} is the offset of the minimum energy from a staggered arrangement. Nonbonded interactions are calculated using a function that includes a repulsive and an attractive (London dispersion) component (Eq. 2.6),

$$E_{\text{nb}} = Ae^{-Bd_{ij}} - Cd_{ij}^{-6} \quad (2.6)$$

where d_{ij} is the distance between the two nuclei and A, B and C are atom based constants discussed later in this book.

More recently a number of additional components have been added to the calculation of the strain energy. Out-of-plane deformation terms E_δ have been included in models of aromatic or sp^2 hybridized systems (Eq. 2.7),

$$E_\delta = \frac{1}{2}k_\delta\delta^2 \quad (2.7)$$

where δ is the angle between the plane defined by three atoms and the vector from the center of these atoms to a fourth bonded atom, and k_δ is the corresponding force constant. Modeling the interaction of metal complexes with biological systems has necessitated the inclusion of electrostatic and hydrogen bonding interaction terms. The electrostatic interactions are modeled based on the Coulomb's law (Eq. 2.7),

$$E_e = \frac{q_i q_j}{\epsilon d_{ij}} \quad (2.8)$$

where q_i and q_j are the partial charges on atoms i and j , ϵ is the dielectric constant and d_{ij} is the interatomic separation. Hydrogen bonding, E_{hb} interactions are generally modeled using a function of the type given in (Eq. 2.9),

$$E_{\text{hb}} = Fd_{ij}^{-12} - Gd_{ij}^{-10} \quad (2.9)$$

where F and G are empirically derived constants that reproduce the energy of a hydrogen bond and d_{ij} is the donor-acceptor distance. The addition of these terms give rise to the revised definition of U_{total} given in (Eq. 2.10),

$$U_{\text{total}} = \sum_{\text{molecule}} (E_b + E_\theta + E_\phi + E_{\text{nb}} + E_\delta + E_e + E_{\text{hb}}) \quad (2.10)$$

The set of functions together with the collection of terms that parameterize them (k_b , r_0 , etc.) is referred to the force field. In some cases force field parameters can be related to experimentally determinable values. For example, the bond stretching force constant k_b is approximately equivalent to the vibrational force constant

derived from an infrared spectrum. However, in general the force field terms are derived empirically with the target of reproducing experimental structures and energy distributions.

Once a model and a force field have been chosen for a particular problem, the goal of molecular mechanics is to find the geometry with the minimum strain energy. This can be achieved by a variety of mathematical techniques described elsewhere in this book. The value of the strain energy is dependent on the force field and therefore has little meaning in absolute terms. However, because isomers have the same bond, bond angle and torsional angle types, strain energies of isomers can be compared to each other and differences correlated with experimentally determined isomer populations.

This has formed the justification of many molecular mechanics studies. In recent studies of more complex systems the primary goal has been to produce reasonable models that allow the investigator to visualize the interactions of metal ions with large molecules. Also, methods where molecular mechanics is used in combination with experimental data to determine molecular structures, for example in solution, are receiving increasing attention.

2.2 Harmonic Functions for Carbon Nanotubes

It has been proved through chemical calculations that harmonic functions provide a reasonable approximation to the potential energy of molecular systems in which the bond length is near its equilibrium position [2]. In this particular formula, the energy terms associated to bond stretching (Eq. 2.11), angle bending (Eq. 2.12) and inversion (Eq. 2.13) are described as [3, 4],

$$U_b = \frac{1}{2} \sum_i K_i (r - r_0)^2 \quad (2.11)$$

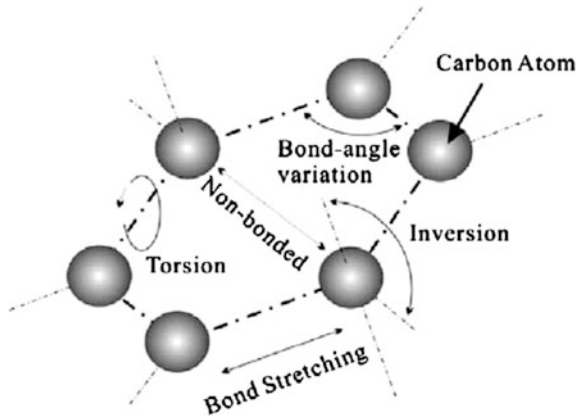
$$U_\theta = \frac{1}{2} \sum_j C_j (\theta - \theta_0)^2 \quad (2.12)$$

$$U_\phi = \frac{1}{2} \sum_k B_k (\phi - \phi_0)^2 \quad (2.13)$$

where $r - r_0$, $\theta - \theta_0$, $\phi - \phi_0$ are the elongation of bond i , variance of bond angle j and inversion angle k , respectively. K_i , C_j and B_k are force constants associated with bond stretching, angle variance and inversion, respectively. Formulation was done by using schematic diagrams as shown in Fig. 2.1.

In such cases, elastic Young's modulus E_n of armchair (n, n) and zigzag (n, 0) CNTs could be expressed as the following,

Fig. 2.1 Schematic illustration of atoms and bonds in CNT



$$E_n = \frac{4\sqrt{3}K}{3\lambda Ka^2/C + 9}, \lambda = \frac{7 - \cos(\pi/n)}{34 + 2\cos(\pi/n)} \quad (2.14)$$

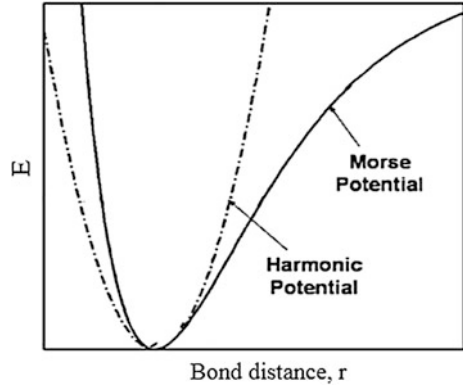
where K , C and a are axial stiffness of the carbon–carbon covalent bond (C–C) (742 nN/nm), bending stiffness resulting from the angular distortion of bond angle (1.42 nN/nm) and bond length, respectively [4].

2.3 Morse Potential Functions for CNTs

It is crucial to note that linear functions are only applicable to characterize material properties under relatively small strain conditions. Obviously, a harmonic function is a good approximation of the bond stretching function near the energy minimum as shown in Fig. 2.2 [3, 5]. However, a more complex function must be used to describe the behavior of a chemical bond far from its equilibrium position such as Morse potential which was used to describe the behavior from equilibrium to bond dissociation [3]. Among presented models, Morse potential function was selected in this study mostly due to its simplicity over many-body potentials such as Brenner function and its compatibility with the finite element method [5–8]. For a SWCNT subjected to axial loadings at large strains, with the proper set of constants, it is possible to simulate all potentials including torsion, inversion, van der Waals and electrostatic interactions [3]. To make the simulation as simple as possible in agreement with [9], those potentials with minor effects were neglected.

After neglecting non effective force fields, the bond total energy could be expressed by the interatomic functions defined by Morse potential. A modified Morse potential function has been established for CNT [6].

Fig. 2.2 The schematic of the Morse and the harmonic potentials [10]



The main improvement was that a bond angle bending potential was added in Morse potential. This modification has been mainly done to facilitate theoretical studies of CNT fracture. It can be written as

$$U = U_{\text{stretch}} + U_{\text{angle}} \quad (2.15)$$

where U_{stretch} and U_{angle} are the bond energy due to bond stretching and bond energy due to bond angle bending. These potentials are shown in Fig. 2.3. In which,

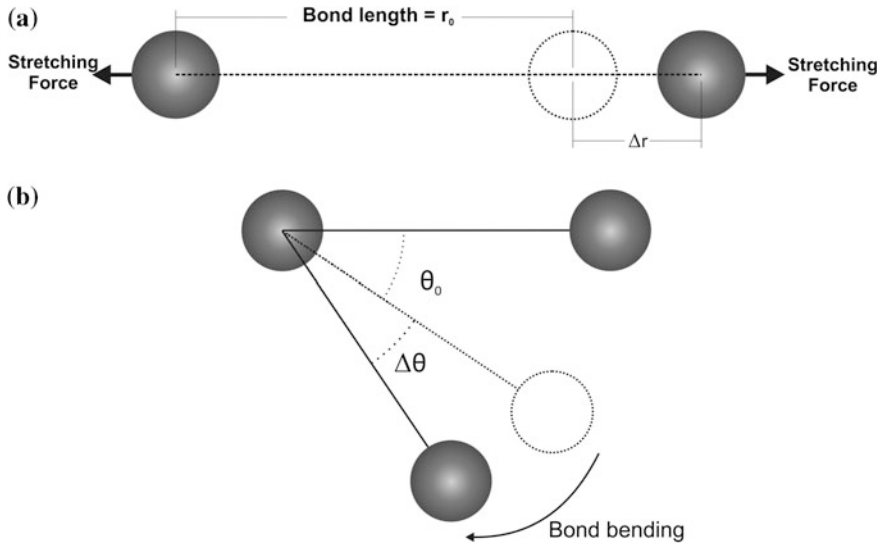


Fig. 2.3 Interatomic interactions according to modified Morse potential for C–C bonds: **a** bond stretching, **b** bond bending

Table 2.1 Associated values of force constants

Symbol	Name	Value
r_0	C–C bond length	1.421×10^{-10} m
θ_0	Bond angle	2.094 rad
D_e	well depth	6.03105×10^{-19} nm
β	Controls the width of the potential	2.625×10^{10} m ⁻¹
k_θ	force constant	0.9×10^{-18} N/rad ²
k_{sexic}	force constant	0.754 rad ⁻⁴

$$U_{\text{stretch}} = D_e \left[\left(1 - e^{-\beta(r-r_0)} \right)^2 - 1 \right] \quad (2.16)$$

$$U_{\text{angle}} = \frac{1}{2} k_\theta (\theta - \theta_0)^2 \left[1 + k_{sexic} (\theta - \theta_0)^4 \right] \quad (2.17)$$

where r and θ are the current bond length and angle of the adjacent bond, respectively. The parameters of the potential are summarized in Table 2.1 [6, 8, 9].

The stretching force and required bending moment to deform C–C bonds were obtained by differentiating bond stretching and angle bending potentials against bond length and bending angle, respectively,

$$F(r) = \frac{\partial U_{\text{stretching}}}{\partial r} = 2\beta D_e \left[1 - e^{-\beta(r-r_0)} \right] e^{-\beta(r-r_0)} \quad (2.18)$$

$$M(\theta) = \frac{\partial U_{\text{bending}}}{\partial \theta} = k_\theta (\theta - \theta_0) \left(1 + 3k_{sexic} (\theta - \theta_0)^4 \right) \quad (2.19)$$

2.4 Potential Interactions for Inorganic Nanotubes

The initial stage in the majority of the atomistic molecular modeling methods (molecular mechanics) is the computation of the energy (Lattice energy in this case). The lattice energy of a crystal can be determined by summing all separate kinds of interactions that may likely occur in a system containing a number of atoms in it [11]. But, the lattice energy calculated is accurate only if higher orders of interactions are also taken into consideration during the calculation process. On the other hand, it is unrealistic to take account of the higher orders of interaction for computation as it will turn out to be exceedingly time consuming [12]. Furthermore since contributions decreases progressively with increasing order of interactions, it is realistic to shorten the increase to two body and three body interactions. The atomic interactions turn out to be weaker as the distance in the middle of the atoms spread wider [11].

Potentials of atoms/molecules are determined using empirical equations (based on interatomic distance) in order to calculate the energy related with the particular atomic interactions. Potentials perform a significant task in defining the precision of the computational modeling investigations [13]. There are various types of chemical bonds occurring in numerous elements for binding the material together, viz. covalent bonds, ionic bonds, metallic bonds, Van der Waals bonds and hydrogen bonds. Every form of bonds will have varied strength. Bonds may also be categorized as intramolecular bonds and intermolecular bonds. Intramolecular bonds keep the atoms together in a molecule. In addition, intramolecular bonds are those that exist between the molecules as in Van der Waals bonding, ionic bonding, covalent bonding, dipole—dipole interaction and hydrogen bonding [11]. In ionic bonding, the ions of opposite charges are attracted to each other. Zirconia (ZrO_2) is an example of ionic bonding. In covalent bonding, the valence electrons are mutual in the middle of atoms not like electron transfer witnessed in ionic bonding. Covalent bonding is witnessed in water and diatomic molecules like O_2 , H_2 etc. These atomic interactions may well be categorized as long and short range interactions [14].

2.4.1 Long Range Interactions

In ionic crystals such as Zr-O, the long range (Coulomb) interactions accounts for most of the total energy of the structure [11]. Considering the ions as specific point charges, the Coulomb's law may be specified as [12]

$$U_{ij}^{\text{Coulomb}} = \frac{q_i q_j}{4\pi\epsilon_0 r_{ij}} \quad (2.20)$$

where U_{ij}^{Coulomb} is the Coulomb's energies, q_i , q_j represent the charges on the pairs of ions, ϵ_0 is the permittivity of free space and r_{ij} is the inter-ionic distance.

The computation of Coulomb energy turns out to be tedious for a 3D bulk material [12]. Exchanges involving ions progressively decrease in the midst of increase in the inter-ionic distances. On the other hand, the amount of ions and therefore the number of interactions among ions increases as the cut-off radius increases. This eventually affects the increase of energy density of interactions with increase in distance [12]. This hindrance may well be fixed by using Ewald summation technique [11, 15, 16], which requires two vital conditions for convergence: (a) Sum of all the charges in the system should be zero (b) Dipole moment should be zero. Ewald summation technique is fundamentally obtained by using Laplace transformation on Eq. 2.22. The Coulomb energy computation occurs in two sections: (a) Real space summation (b) Reciprocal space summation. Real space summation section converges promptly and the reciprocal space summation section decays rapidly. A Gaussian charge distribution is included and deducted from each ion. The expression for the approximation of Coulomb energy (U^{CE}) as the sum

total of inputs from real space (U^{real}), reciprocal space ($U^{\text{reciprocal}}$) and self-energy ($U^{\text{selfenergy}}$) of the ions is specified by [13]:

$$U^{CE} = \frac{1}{2} \sum_{i=1}^N \sum_{j=1}^N \frac{q_i q_j}{r_{ij}} \text{erfc}(\eta^{\frac{1}{2}} r_{ij}) + \frac{1}{2} \sum_{i=1}^N \sum_{j=1}^N \sum_G \frac{4}{\pi} q_i q_j \exp(iGr_{ij}) \frac{\exp\left(\frac{G^2}{4\pi}\right)}{G^2} - \sum_{i=1}^N q_i^2 \left(\frac{\eta}{\pi}\right)^{0.5} \quad (2.21)$$

$$U^{CE} = U^{\text{real}} + U^{\text{reciprocal}} - U^{\text{selfenergy}} \quad (2.22)$$

From Eq. 2.22, q represents the charge of the ion, G is equal to the reciprocal lattice vector, V is the unit cell volume, N is the number of atoms in the system and η represents the ratio of task among real and reciprocal space.

2.4.2 Short Range Interactions

Short range (non-Coulombic) interactions perform a critical part in approximating the position and profile of the minimum energy [11]. Mostly, the two body terms influence the short range interactions. Two body terms consist of interactions amongst atoms that are ions or attached. The three most prevalently used two-body potentials are Buckingham potential, Lennard-Jones potential and Morse potential [13]. The expressions for the potentials are given by:

$$U_{ij}^{\text{Buckingham}} = A \exp\left(\frac{-r_{ij}}{\rho}\right) - \frac{C_6}{r_{ij}^6} \quad (2.23)$$

$$U_{ij}^{\text{Lennard-Jones}} = \frac{C_m}{r_{ij}^m} - \frac{C_6}{r_{ij}^6} \quad (2.24)$$

$$U_{ij}^{\text{Morse}} = D_e \left[(1 - \exp(-a(r - r_0)))^2 \right] - 1 \quad (2.25)$$

where, r_{ij} is the inter-atomic distance and all the other terms are the parameters of the potential.

The Buckingham potential and Lennard-Jones potential include comparable terms in Eqs. (2.23) and (2.24) i.e., a repulsive part and attractive part. The C_6 portion obtained in all the potentials is the attractive part of the potential and it is not required to model in relation to ionic bonds [17]. Thus for ZrO_2 , the potential energy is obtained as a sum of two-body interactions of the form [11]:

Table 2.2 Parameters for atomic interactions in ZrO₂ [11]

Pair	A _{ij} (eV)	ρ _{ij} (Å)	C _{ij} (eVÅ ⁻⁶)
Zr-O	985.87	0.3760	0.0
Zr-Zr	22764.3	0.1490	27.89
O-O	0.0	0.0	0.0

$$U = U^{\text{bonded}} + U^{\text{nonbonded}}$$

$$U = A \exp\left(\frac{-r_{ij}}{\rho}\right) - \frac{C_6}{r_{ij}^6} + \frac{q_i q_j}{4\pi\epsilon_0 r_{ij}} \quad (2.26)$$

Parameters in Eq. 2.26 for ZrO₂ have been developed by empirical method [11, 18] and are indicated in Table 2.2.

The electric permittivity of vacuum, $\epsilon_o = 0.55263614 \times 10^{-12} \text{ C}^2\text{eV}^{-1}\text{\AA}^{-1}$; $q_{\text{Zr}} = 4e$; $q_{\text{O}_2} = -2e$; where e is the magnitude of electronic charge, $1.602 \times 10^{-19} \text{ C}$ [11, 18]. The Morse potential is used for atomic interactions where covalent bond dominates in the total energy for the system such CNT, BN and others [17].

References

1. D.W. Brenner, Empirical potential for hydrocarbons for use in simulating the chemical vapor deposition of diamond films. *Phys. Rev. B* **42**, 9458–9471 (1990)
2. N.L. Allinger, *Molecular Structure: Understanding Steric and Electronic Effects from Molecular Mechanics* (Wiley, 2010)
3. T. Chang, H. Gao, Size-dependent elastic properties of a single-walled carbon nanotube via a molecular mechanics model. *J. Mech. Phys. Solids* **51**, 1059–1074 (2003)
4. G.M. Odegarda, T.S. Gatesb, L.M. Nicholsonc, K.E. Wised, Equivalent-continuum modeling of nano-structured materials. *Compos. Sci. Technol* **62**, 1869–1880 (2002)
5. H. Wan, F. Delale, A structural mechanics approach for predicting the mechanical properties of carbon nanotubes. *Meccanica* **45**, 43–51 (2010)
6. T. Belytschko, S.P. Xiao, G.C. Schatz, R.S. Ruoff, Atomistic simulations of nanotube fracture. *Phys. Rev. B* **65**, 235–430 (2002)
7. J. Xiao, B. Gama, J. Gillespiejr, An analytical molecular structural mechanics model for the mechanical properties of carbon nanotubes. *Int. J. Solids Struct.* **42**, 3075–3092 (2005)
8. K. Tserpes, P. Papanikos, G. Labeas, S. Pantelakis, Multi-scale modeling of tensile behavior of carbon nanotube-reinforced composites. *Theoret. Appl. Fract. Mech.* **49**, 51–60 (2008)
9. M. Rossi, M. Meo, On the estimation of mechanical properties of single-walled carbon nanotubes by using a molecular-mechanics based FE approach. *Compos. Sci. Technol.* **69**, 1394–1398 (2009)
10. G. Cao, X. Chen, J.W. Kysar, Thermal vibration and apparent thermal contraction of single-walled carbon nanotubes. *J. Mech. Phys. Solids* **54**, 1206–1236 (2006)
11. M.A. Caravaca, J.C. Mino, V.J. Pérez, R.A. Casali, C.A. Ponce, Ab initio study of the elastic properties of single and polycrystal TiO₂, ZrO₂ and HfO₂ in the cotunnite structure. *J. Phys.: Condens. Matter* **21**(1), (2009)
12. M.C. Payne, M.P. Teter, D.C. Allan, T.A. Arias, J.D. Joannopoulos, Iterative minimization techniques for ab initio total-energy calculations: molecular dynamics and conjugate gradients. *Rev. Mod. Phys.* **64**(4), 1045 (1992)

13. G.V. Lewis, C.R.A. Catlow, Potential models for ionic oxides. *J. Phys. C: Solid State Phys.* **18** (6), 1149–1156 (1985)
14. D. Fang, Z. Luo, S. Liu, T. Zeng, L. Liu, J. Xu, W. Xu, Photoluminescence properties and photocatalytic activities of zirconia nanotube arrays fabricated by anodization. *Opt. Mater.* **35** (7), 1461–1466 (2013)
15. S.J. Clark, M.D. Segall, C.J. Pickard, P.J. Hasnip, M.I. Probert, K. Refson, M.C. Payne, First principles methods using CASTEP. *Z. Kristallogr.* **220**, 567–570 (2005)
16. M.C. Payne, M.P. Teter, D.C. Allan, T.A. Arias, J.D. Joannopoulos, Iterative minimization techniques for ab initio total-energy calculations: molecular dynamics and conjugate gradients. *Rev. Mod. Phys.* **64**(4), 1045 (1992)
17. A.R. Yavari, J.J. Lewandowski, J. Eckert, Mechanical properties of bulk metallic glasses. *MRS Bull.* **32**(08), 635–638 (2007)
18. A. Dwivedi, A.N. Cormack, A computer simulation study of the defect structure of calcia-stabilized zirconia. *Philos. Mag. A* **61**(1), 1–22 (1990)

Finite Element Modeling of Nanotube Structures

Linear and Non-linear Models

Awang, M.; Mohammadpour, E.; Muhammad, I.D.

2016, XIII, 212 p., Hardcover

ISBN: 978-3-319-03196-5